

Shang-ke Chen,^a Kui Wang,^b
 Yuhuan Liu^{b*} and Xiaopeng Hu^{a*}

^aSchool of Pharmaceutical Sciences, Sun Yat-sen University, Higher Education Mega Center, Guangzhou, Guangdong 510006, People's Republic of China, and ^bSchool of Life Sciences, Sun Yat-sen University, Guangzhou, Guangdong 510275, People's Republic of China

Correspondence e-mail:
 lsslyh@mail.sysu.edu.cn,
 huxpeng@mail.sysu.edu.cn

Received 12 December 2011
 Accepted 21 April 2012

Crystallization and preliminary X-ray analysis of a novel halotolerant feruloyl esterase identified from a soil metagenomic library

Feruloyl esterase cleaves the ester linkage formed between ferulic acid and polysaccharides in plant cell walls and thus has wide potential industrial applications. A novel feruloyl esterase (EstF27) identified from a soil metagenomic library was crystallized and a complete data set was collected from a single cooled crystal using an in-house X-ray source. The crystal diffracted to 2.9 Å resolution and belonged to space group $P2_12_12_1$, with unit-cell parameters $a = 94.35$, $b = 106.19$, $c = 188.51$ Å, $\alpha = \beta = \gamma = 90.00^\circ$. A Matthews coefficient of 2.55 Å³ Da⁻¹, with a corresponding solvent content of 51.84%, suggested the presence of ten protein subunits in the asymmetric unit.

1. Introduction

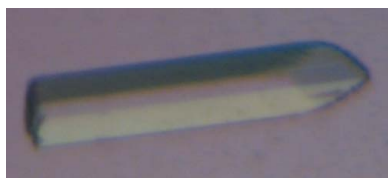
Ferulic acid esterases (FAEs; EC 3.1.1.73) represent a subclass of carboxylic acid esterases which catalyse the hydrolysis of the ester linkages of ferulic acid/ ρ -coumaric acid and diferulates present in plant cell walls. Working in synergy with xylanases, FAEs degrade the plant cell wall and release polysaccharides and ferulic acid (Goldstone *et al.*, 2010; Williamson *et al.*, 1998).

FAEs have broad potential industrial applications. In the paper-making industry, raw plant materials could be treated with FAEs and other enzymes to increase the alkaline solubility of the product and to reduce the use of chlorine in the bleaching process (Record *et al.*, 2003; Sigoillot *et al.*, 2005). In the feed industry, FAEs could be used to improve feed efficiency (Guglielmetti *et al.*, 2008). In bio-energy, FAEs could increase the yield of fermentable sugars such as glucose and xylose (Tabka *et al.*, 2006). In biological synthesis, FAEs could be used to convert liposoluble compounds to water-soluble substances (Topakas *et al.*, 2005). FAEs also provide an effective and efficient way to produce ferulic acid, which exhibits broad antioxidant, antimicrobial, anti-inflammatory, antithrombosis and anticancer properties (Koseki, Fushinobu *et al.*, 2009; Mathew & Abraham, 2004).

Around 50 FAEs with different properties have been identified from microorganisms (Koseki, Fushinobu *et al.*, 2009; Abokitse *et al.*, 2010). Most of these enzymes have the α/β -hydrolase structure with a Ser-His-Asp catalytic triad. However, owing to varying weaknesses, none of these FAEs have been successfully employed in industry (Crepin *et al.*, 2003; Koseki, Hori *et al.*, 2009; Moukouli *et al.*, 2008; Shin & Chen, 2007).

EstF27 was isolated from a metagenomic library from agricultural soil (Sang *et al.*, 2011). A protein *BLAST* search against the NCBI database revealed that EstF27 (accession No. ADU32684) shows moderate identity to a putative esterase/lipase from *Cardiobacterium hominis* ATCC15826 (ZP_05706399; 47% identity). According to the PROSITE database (<http://www.expasy.ch/prosite/>), EstF27 has a LIPASE_GDXG_HIS pattern (PS01173). A phylogenetic analysis of EstF27, FAEs and several hypothetical FAEs revealed that EstF27 is adjacent to FAEs (Sang *et al.*, 2011).

The specific activity of EstF27 towards *p*-nitrophenyl ferulate was 21.7 ± 1.7 U mg⁻¹, which is much higher than those of other FAEs (3.375 U mg⁻¹ for FAE from *Eleusine coracana*, 9.0 ± 0.1 U mg⁻¹ for FAE-1 from *Aspergillus niger* and 11.2 ± 0.02 U mg⁻¹ for FAE-2 from *A. niger*; Latha *et al.*, 2007; Hegde & Muralikrishna, 2009). EstF27 also exhibits several novel features, including halotolerance (retaining more than 50% activity after 96 or 120 h incubation in the



presence of 3 M KCl or 5 M NaCl), alkali tolerance (being stable over the relatively large pH range 5–10) and highly soluble expression in *Escherichia coli*.

We are interested in investigating the three-dimensional structure of EstF27 as a basis for protein engineering. The three-dimensional structure of EstF27 should provide new insights into its catalytic mechanism, halotolerance and other properties. This paper presents the initial steps towards three-dimensional structure determination of EstF27.

2. Materials and methods

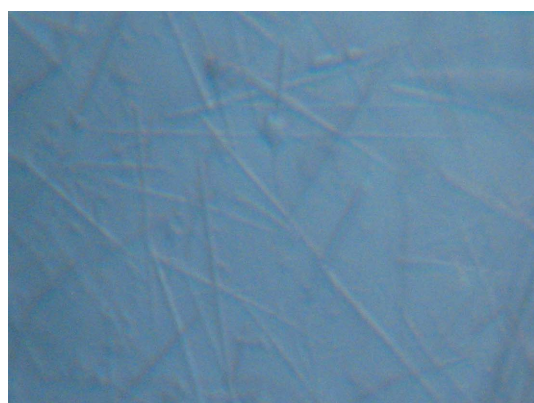
2.1. Preparation and concentration of the sample

The original cloning of full-length *EstF27* from a soil metagenomic library (GenBank accession No. HQ241478) has been described previously (Sang *et al.*, 2011). For crystallization, *EstF27* was subcloned into expression vector pEQ-30 between *Bam*HI and *Hind*III restriction sites, with 12 additional amino acids (MRGSH-HHHHHGS–), including a hexahistidine tag, at the N-terminus. The

resultant plasmids were transformed into *E. coli* strain BL21 (DE3) cells for overexpression and the cells were cultured at 310 K in Luria–Bertani medium containing 50 mg l⁻¹ ampicillin (Sigma, USA). When the optical density at 600 nm (OD₆₀₀) reached 0.8, the cultures were induced with 0.1 mM isopropyl β-D-1-thiogalactopyranoside and maintained at 289 K for 20 h. The cells were then harvested by centrifugation at 4800 rev min⁻¹ for 25 min at 277 K and resuspended in cold lysis buffer (25 mM Tris–HCl pH 8.0, 500 mM NaCl, 10 mM imidazole, 1 mM β-mercaptoethanol, 1% Tween-20, 10% glycerol, 1 mg ml⁻¹ lysozyme). The suspension was sonicated and the soluble proteins in the supernatant were recovered by centrifugation at 45 000 rev min⁻¹ for 35 min at 277 K. The supernatant was loaded onto a nickel-chelating HisTrap FF column (GE Healthcare, USA) which had been pre-equilibrated with binding buffer (lysis buffer without lysozyme). The column was washed with binding buffer followed by washing buffer (50 mM NaCl, 50 mM Tris–HCl pH 8.0, 10–50 mM imidazole, 1 mM β-mercaptoethanol, 10% glycerol). The recombinant protein was eluted with elution buffer (50 mM NaCl, 50 mM Tris–HCl pH 8.0, 250 mM imidazole, 1 mM β-mercaptoethanol, 10% glycerol). The purified protein was ultrafiltered and concentrated using Amicon Ultra-10 (Millipore, USA) in storage buffer consisting of 200 mM NaCl, 10 mM HEPES pH 7.5, 5 mM dithiothreitol, 10% glycerol prior to crystallization setup. The purity of the recombinant protein was greater than 98%.

2.2. Crystallization

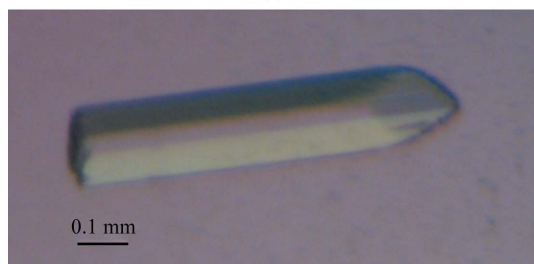
Initial crystallization screening was performed manually using Crystal Screen and Crystal Screen 2 (Hampton Research) by vapour diffusion in hanging drops at 289 K in 24-well plates. Each drop consisted of 2 μl 15 mg ml⁻¹ protein solution and 2 μl crystallization cocktail and was equilibrated against 500 μl reservoir solution. Several conditions were found to give tiny acicular crystals in one or two weeks; condition No. 15 of Crystal Screen (0.2 M ammonium



(a)



(b)



(c)

Figure 1

(a) Acicular crystals of EstF27. (b) Fern-like crystals of EstF27. (c) Rod-shaped crystal of EstF27 with typical dimensions of 0.12 × 0.12 × 0.74 mm.

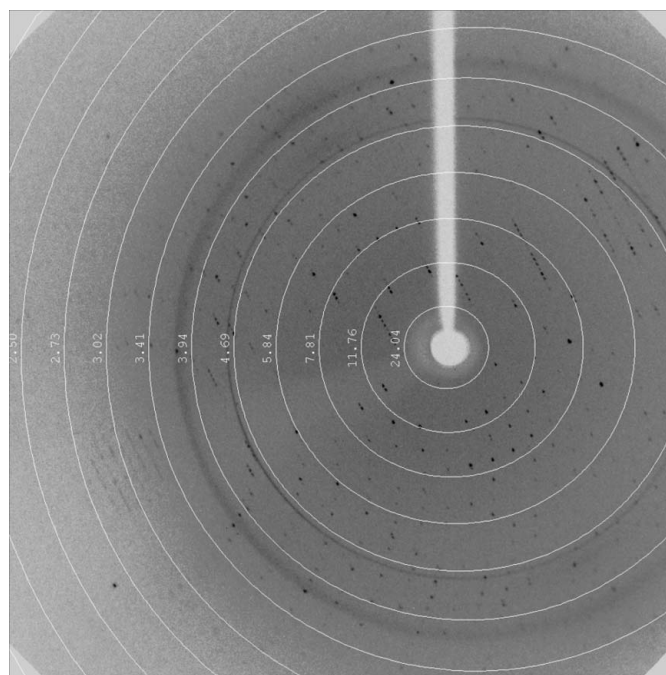


Figure 2

A typical diffraction pattern of an EstF27 crystal. The exposure time was 150 s, the crystal-to-detector distance was 120.0 mm and the oscillation range per frame was 0.25°. The diffraction image was collected on a 165 mm Onyx CCD detector.

sulfate, 30% PEG 8000, 0.1 M sodium cacodylate pH 6.5) was further optimized by varying the precipitant, salt, buffer, pH and additives. The optimum condition consisted of 0.2 M ammonium sulfate, 26% PEG 4000, 0.1 M sodium cacodylate pH 6.5, 4% (w/v) benzamidine-HCl. Rod-shaped crystals were obtained in two weeks at 289 K (Fig. 1).

2.3. X-ray diffraction data collection

For X-ray diffraction experiments, a rod-shaped crystal was picked up from the crystallization drop using a nylon loop, transferred into 30 μ l dehydrating solution consisting of 0.2 M ammonium sulfate, 36% PEG 4000, 0.1 M sodium cacodylate pH 6.5, 4% (w/v) benzamidine-HCl, 10% glycerol and dehydrated in air for 7–8 h. The crystal was then flash-cooled in a dry nitrogen-gas stream at 100 K. A complete X-ray diffraction data set was collected at a wavelength of 1.5418 Å using an in-house Oxford Diffraction Xcalibur Nova diffractometer operating at 50 kV and 0.8 mA. The exposure time and crystal oscillation angle were set to 150 s and 0.25°, respectively. The crystal-to-detector distance was maintained at 120 mm. The crystal diffracted X-rays to 2.9 Å resolution. A total of 572 images were recorded using a 165 mm Onyx CCD detector. The data were processed and scaled using *CrysAlis^{Pro}* (v.1.171.33.49; Oxford Diffraction) and programs from the *CCP4* suite (Winn *et al.*, 2011). A typical diffraction image of an EstF27 crystal is shown in Fig. 2.

3. Results and discussion

The concentrated recombinant EstF27 crystallized in various shapes (plates, rods, needles and dendrites) using the hanging-drop vapour-diffusion method at 289 K with a wide range of reservoir solutions comprising 24–34% PEG (PEG 3350, 4000, 6000 or 8000), 0.1 M Tris pH 8.0 or 0.1 M sodium cacodylate pH 6.5, 0.2 M Li₂SO₄ or 0.2 M ammonium sulfate. However, these crystals were too small for diffraction testing. By careful refinement, large rod-shaped crystals

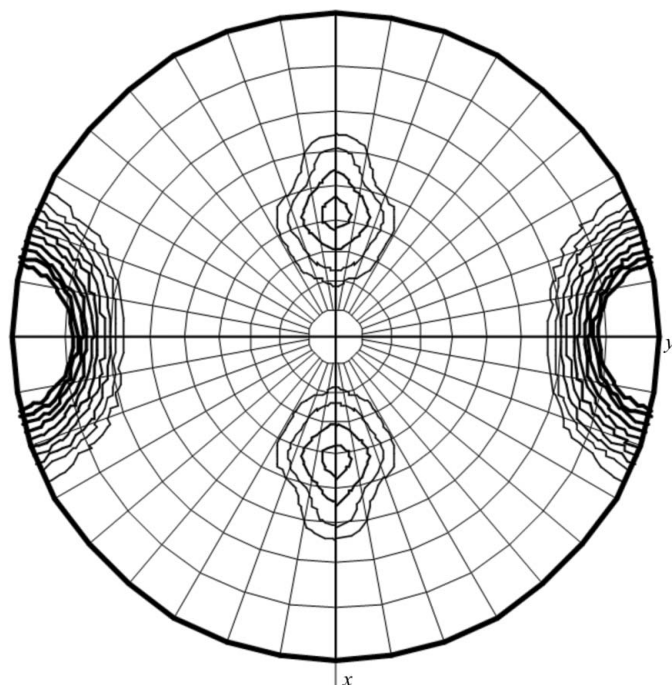


Figure 3
Plot of the $\chi = 72^\circ$ section of a self-rotation function from *MOLREP* (*CCP4* suite).

Table 1

Comparison of data-collection statistics.

Value in parentheses are for the highest resolution shell.

Crystallization conditions	0.2 M ammonium sulfate, 26% PEG 4000, 0.1 M sodium cacodylate pH 6.5, 4% (w/v) benzamidine-HCl
Wavelength (Å)	1.5418
Temperature (K)	100
Resolution range (Å)	24.26–2.90 (3.06–2.90)
Space group	<i>P</i> ₂ <i>1</i> <i>2</i> ₁
Unit-cell parameters (Å, °)	<i>a</i> = 94.35, <i>b</i> = 106.19, <i>c</i> = 188.51, $\alpha = \beta = \gamma = 90.00$
Observed reflections	142308 (13956)
Unique reflections	42403 (6048)
Data completeness (%)	99.3 (98.5)
Multiplicity	3.4 (2.3)
$\langle I/\sigma(I) \rangle$	6.1 (2.1)
<i>R</i> _{merge} † (%)	0.131 (0.377)
Matthews coefficient (Å ³ Da ⁻¹)	2.55
Solvent content (%)	51.84

† $R_{\text{merge}} = \frac{\sum_{hkl} \sum_i |I_i(hkl) - \langle I(hkl) \rangle|}{\sum_{hkl} \sum_i I_i(hkl)}$, where $I_i(hkl)$ are the observed diffraction-intensity values of unique reflection hkl and $\langle I(hkl) \rangle$ is the mean value of $I(hkl)$ for all i measurements.

were finally obtained by mixing 2 μ l protein solution (15 mg ml⁻¹) with 2 μ l well buffer consisting of 0.2 M ammonium sulfate, 26% PEG 4000, 0.1 M sodium cacodylate, 4% (w/v) benzamidine-HCl pH 6.5. However, these crystals diffracted very poorly. Post-crystallization treatments such as annealing and soaking the crystals in a more concentrated precipitant solution were therefore performed. Crystal cross-linking with glutaraldehyde failed, but crystal dehydration by equilibrating the crystals in dehydration solution in air for around 8 h dramatically improved the diffraction quality from around 8 to 2.9 Å resolution on an in-house X-ray source.

A complete X-ray diffraction data set was collected from a single treated crystal. It was processed using *CrysAlis^{Pro}* (v.1.171.33.49; Oxford Diffraction) and scaled using *SCALA* from the *CCP4* suite (Winn *et al.*, 2011) at a cutoff of 2.9 Å. The crystal belonged to space group *P*₂*1**2*₁, with unit-cell parameters *a* = 94.35, *b* = 106.19, *c* = 188.51 Å, $\alpha = \beta = \gamma = 90.00^\circ$. The data-collection and processing statistics are summarized in Table 1. The calculated Matthews coefficient (V_M ; Matthews, 1968) of 2.55 Å³ Da⁻¹ suggested the presence of ten monomers in the asymmetric unit (51.84% solvent content). Calculation of a self-rotation function with *MOLREP* from the *CCP4* suite also indicated the presence of a noncrystallographic fivefold axis (Fig. 3) and implied the assembly of five molecules. A fragment of a thermophilic *p*-nitrobenzyl esterase (PDB entry 1c7i; Spiller *et al.*, 1999) shares the highest sequence identity to EstF27 in the PDB (32.3% identity) and was used as a molecular-replacement (MR) search model. *MOLREP* resulted in solutions with *R* factors between 0.55 and 0.60 and low scores of about 2. Further refinement could not be performed. MR was also attempted in lower symmetry space groups and with *Phaser*, *MrBUMP* and *BALBES*, but no solutions were obtained. Using the crystal structure of the type A FAE from *A. niger* (PDB entry 1uwc; McAuley *et al.*, 2004), which shares 38.6% similarity and 15.0% identity with EstF27, as a search model was also unsuccessful. The oligomeric state, such as the possible pentameric structure, and deviations between the search models and the actual structure could be responsible for the unsuccessful MR trials. A more systematic approach is being undertaken and we are also working on obtaining a solution using the MAD method.

The authors thank the National Natural Science Foundation of China (31170117), the National Marine Research Special Funds for Public Welfare Projects of China (201205020-07), the Major

Science and Technology Projects of Guangdong Province, China (2011A080403006), the Science and Technology Plan Project of Guangdong Province (2010A080403005), the National High Technology Research and Development Program of China (863 Program; 2007AA10Z308) and the Research (Innovative) Fund of Laboratory Sun Yat-sen University (YJ201027) for financial support.

References

- Abokitse, K., Wu, M., Bergeron, H., Grosse, S. & Lau, P. C. (2010). *Appl. Microbiol. Biotechnol.* **87**, 195–203.
- Crepin, V. F., Faulds, C. B. & Connerton, I. F. (2003). *Biochem. J.* **370**, 417–427.
- Goldstone, D. C., Villas-Bôas, S. G., Till, M., Kelly, W. J., Attwood, G. T. & Arcus, V. L. (2010). *Proteins*, **78**, 1457–1469.
- Guglielmetti, S., De Noni, I., Caracciolo, F., Molinari, F., Parini, C. & Mora, D. (2008). *Appl. Environ. Microbiol.* **74**, 1284–1288.
- Hegde, S. & Muralikrishna, G. (2009). *World J. Microbiol. Biotechnol.* **25**, 1963–1969.
- Koseki, T., Fushinobu, S., Ardiansyah, Shirakawa, H. & Komai, M. (2009). *Appl. Microbiol. Biotechnol.* **84**, 803–810.
- Koseki, T., Hori, A., Seki, S., Murayama, T. & Shiono, Y. (2009). *Appl. Microbiol. Biotechnol.* **83**, 689–696.
- Latha, G., Srinivas, P. & Muralikrishna, G. (2007). *J. Agric. Food Chem.* **55**, 9704–9712.
- Mathew, S. & Abraham, T. E. (2004). *Crit. Rev. Biotechnol.* **24**, 59–83.
- Matthews, B. W. (1968). *J. Mol. Biol.* **33**, 491–497.
- McAuley, K. E., Svendsen, A., Patkar, S. A. & Wilson, K. S. (2004). *Acta Cryst. D* **60**, 878–887.
- Moukoulis, M., Topakas, E. & Christakopoulos, P. (2008). *Appl. Microbiol. Biotechnol.* **79**, 245–254.
- Record, E., Asther, M., Sigoillot, C., Pagès, S., Punt, P. J., Delattre, M., Haon, M., van den Hondel, C. A. M. J. J., Sigoillot, J.-C., Lesage-Meessen, L. & Asther, M. (2003). *Appl. Microbiol. Biotechnol.* **62**, 349–355.
- Sang, S. L., Li, G., Hu, X. P. & Liu, Y. H. (2011). *J. Mol. Microbiol. Biotechnol.* **20**, 196–203.
- Shin, H.-D. & Chen, R. R. (2007). *Appl. Microbiol. Biotechnol.* **73**, 1323–1330.
- Sigoillot, C., Camarero, S., Vidal, T., Record, E., Asther, M., Pérez-Boada, M., Martínez, M. J., Sigoillot, J.-C., Asther, M., Colom, J. F. & Martínez, A. T. (2005). *J. Biotechnol.* **115**, 333–343.
- Spiller, B., Gershenson, A., Arnold, F. H. & Stevens, R. C. (1999). *Proc. Natl Acad. Sci. USA*, **96**, 12305–12310.
- Tabka, M. G., Herpoël-Gimbert, I., Monod, F., Asther, M. & Sigoillot, J.-C. (2006). *Enzyme Microb. Technol.* **39**, 897–902.
- Topakas, E., Vafiadi, C., Stamatis, H. & Christakopoulos, P. (2005). *Enzyme Microb. Technol.* **36**, 729–736.
- Williamson, G., Kroon, P. A. & Faulds, C. B. (1998). *Microbiology*, **144**, 2011–2023.
- Winn, M. D. *et al.* (2011). *Acta Cryst. D* **67**, 235–242.